On VNA Calibration and De-embedding Considerations for Quantum Computing-related and Other Millikelvin Measurements

Jon Martens

[Summary] Increasingly, network analysis measurements are required in millikelvin environments for quantum computing and other applications. For thermal load and related reasons, the path insertion losses to the reference plane may exceed 50 dB raising important questions about the measurement architecture as well as the required calibration and de-embedding methods. The use of reversed local reflectometer structures can help as long as attention is paid to receiver linearity. As calibration/de-embedding standards interfacing is more complicated, assessment of repeatability takes on added importance and the use of partial-information second-tier methods may be useful.

1 Introduction

Significant worldwide investment is being applied to quantum computing and related applications[1)-3)]. Some superconducting implementations of these structures, as well as other current scientific inquiries[4)-6)], make use of millikelvin temperatures for operation and, because of the use of microwave sensing and stimulus operations, S-parameter measurements of components and subsystems are often needed. Since mK S-parameters are rarely predictable based on room temperature data, measurements in the environment of interest are often required. Due to limited cooling capacity at these temperatures, thermal isolation is of paramount importance including the heat load that may be transmitted by microwave cables[7)]. As a result, large attenuators are needed in these RF paths as suggested by the block diagram in Figure 1.

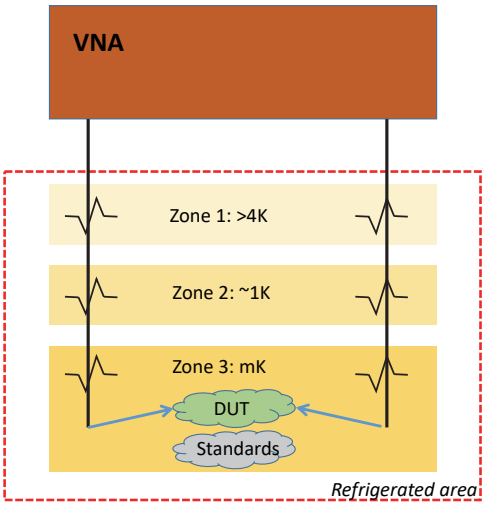

Figure 1 A common cryogenic measurement configuration with multiple refrigeration stages and high required insertion loss.

One can imagine performing a VNA calibration at the room temperature plane and then trying to de-embed the loss to the DUT reference plane, but the loss levels make that untenable in many cases (not to mention the temperature gradient experienced by the cable/attenuation assembly affecting the parameters of that path). A simple well-matched transmission measurement may be possible to execute but any return loss measurement (or the use of match correction in a transmission measurement) will be subject to repeatability sensitivity because of the losses. As an example, a DUT with about 25 dB return loss was measured with the room-temperature calibration approach and then the 60 dB loss path was connected. Although the de-embedding characterization was reasonably accurate, the net result was not (see Figure 2). A characterization transfer error (including repeatability) of less than 10^{-6} in transmission would be needed for reasonable results in this case and that is generally not practically achievable.

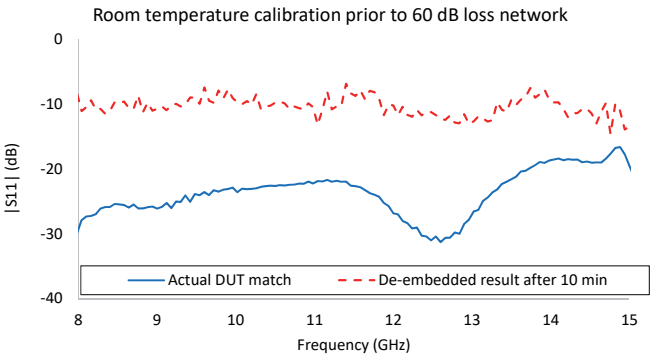

Figure 2 De-embedding high loss networks can result in high sensitivities. The lower repeatabilities in cryogenic measurements can lead to poor stability when de-embedding is done classically.

As a result of this, different approaches have been taken including moving part of the signal separation hardware to the cryogenic level and employing different calibration and de-embedding approaches[8]. This paper will look at some of these variations with an emphasis on net sensitivities to repeatability and other uncertainty drivers.

2 Signal separation configurations

Placing directional couplers (or circulators in cases of some reflection-only measurements) in the cryogenic zone is a common method[e.g., 7]. An additional issue is the low signal levels involved due to the required attenuation so the reverse coupler configuration (see Figure 3) with the addition of a receive-side LNA has been popular and has been discussed extensively in the literature[e.g., 9]. The drive power is reduced but the effective raw directivity of the setup is the same as for a standard coupler configuration and, generally, stability is unaffected.

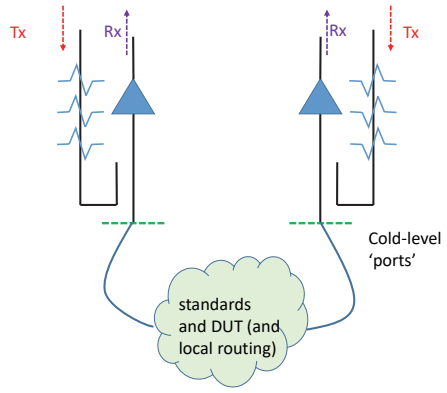

Figure 3 A common signal separation configuration for millikelvin measurements.

This reversed coupler change along with the introduction of a (potentially high gain) LNA does raise some questions about linearity that warrant study since, although the signal levels are low, some LNA technologies/structures may show nonlinear behavior at relatively low levels[e.g., 10]. While nonlinearity can have many manifestations, two aspects of interest are simple compression and nonlinear input match. Compression, of course, represents a level-dependent complex gain but, importantly, can have a more nuanced effect on a calibration[11]. Consider the measurement of a mismatched structure (Figure 4). If the calibration is done in a fully linear region but the measurement is done while the instrument is compressed to about 0.5 dB, the measurement shows some distortion at the highest reflected signal levels. If the calibration is also done while compressed, the result may be distorted at a variety of DUT signal levels and there may be compensation in places.

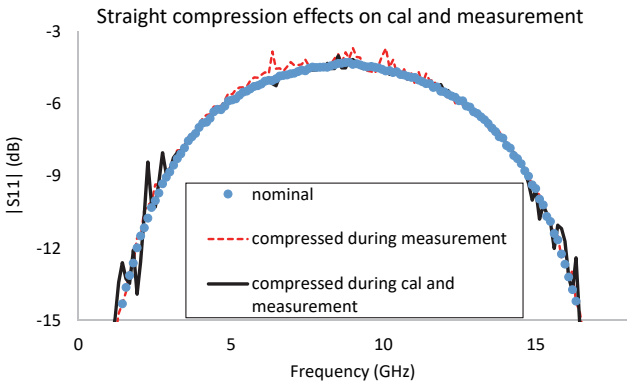

Figure 4 Compression during calibration steps can result in a distorted 'map' of error coefficients.

Nonlinear match can be an issue since port match then becomes dynamic and this is not anticipated by most correction models. Also, in the reverse coupler configuration, that dynamic match is more exposed to the DUT. The match behavior of two example LNAs are shown in Figure 5 expressed as a vector difference from the low power match. These LNAs were designed for high gain and optimized for noise performance. An example of the effects on one of the error coefficients (source match) is shown in Figure 6. The source match coefficient varies rapidly with frequency since not only does the amplifier distortion vary with frequency but so does the absolute mismatch level.

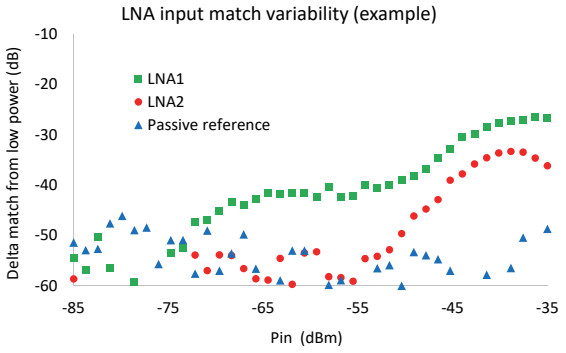

Figure 5 Example LNA nonlinear input match plotted relative to the low power values. The result for a passive device is included as a reference.

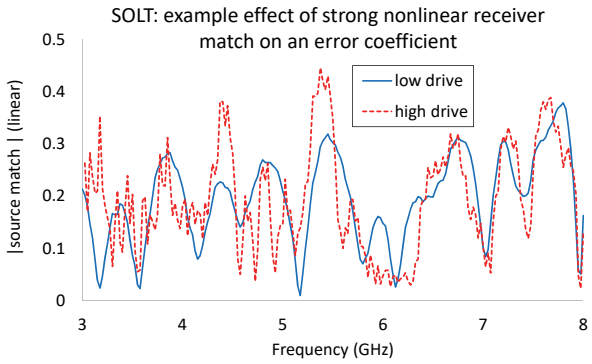

Figure 6 Example effect of LNA nonlinear match on a short-open-load calibration error term.

The net result of these two nonlinear effects on DUT match (in particular) can be significant. The vector delta error (in dB) from the correct result is plotted vs, drive power in Figure 7 for an example low loss device.

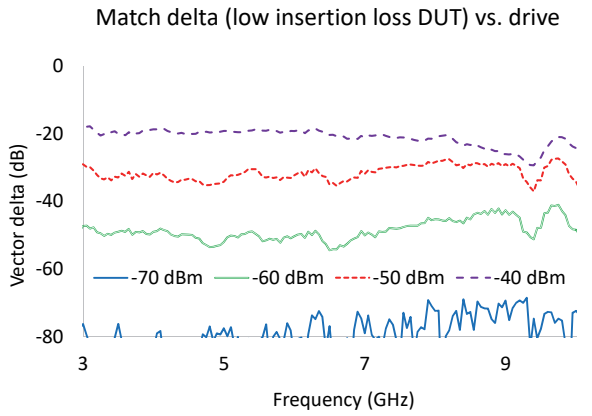

Figure 7 Example net effect of LNA nonlinearity on a DUT match measurement.

The sensitivity behaviors to the receive-side nonlinearities do vary with the calibration algorithm. In the thru-reflect-line (TRL) family, for example, directivity is derived from measurements of return loss when a transmission line is connected. Thus, if there are significant differences in loss between the lines, nonlinear effects will change and the directivity error term can be strongly affected. In the short-open-load family, it is more often that the source match and tracking terms that are affected.

The net system design result is that the potential impact of receiver nonlinearities must be weighed against the impact of poor signal-to-noise ratio. This is, of course, the same for any receiver design but the absolute levels have shifted lower from those in conventional VNA setups.

3 Calibration algorithmic choices

Based on section 2, there is value in placing the 'test port' in the cryogenic environment but this means all calibration and de-embedding standards must also be there which implies some switching is needed. By necessity, this may mean the use of electromechanical switching which does have repeatability implications. Transmission magnitude and phase as well as reflection are affected and include both random and sequential repeatability terms. Figure 8 shows vector difference match repeatability over 20 cycles and, while there is a general trend from cycle-to-cycle, there are occasional outliers due to random landing positions of the switching contact.

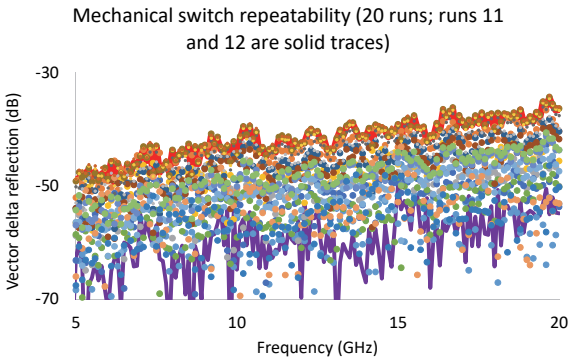

Figure 8 Example mechanical switch repeatability (match in a vector-delta sense).

An additional complication at cryogenic temperatures is the behavior of load standards as the resistive materials used (e.g., tantalum compounds) change behavior at low temperature and may even become superconducting. While this behavior can be characterized, that may not overcome a near-singularity in the calibration. Overdetermined, non-load-based methods may be of interest and these include mSSS[e.g., 12] and mTRL[e.g., 13]. The former uses offset shorts and the sensitivity to individual repeatability issues can be reduced by using extra standards. An example of this sensitivity reduction is shown in Figure 9 where five and three (the minimum) shorts are used and a problem with the standards' behavior (5% error in the offset lengths of one standard) was deliberately introduced. While the distortion caused significant errors in a termination measurement in both cases, the overdetermined calibration was less affected. Additional shorts also enable the calibration to cover a wider bandwidth[12].

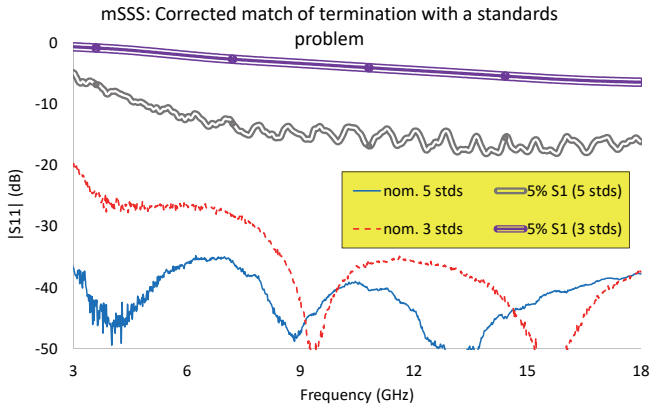

Figure 9 A non-load-based calibration with overdetermined (short) standards may be attractive. Here the effect of an offset length error on the measurement of a termination is shown for conventional (SSS, 3 stds) and overdetermined (5 stds) calibrations.

The more common overdetermined method is mTRL where a number of transmission lines are used instead and the consistent characteristic impedance of these lines forms the reference impedance. Again, additional lines also increase the available bandwidth of the calibration[13]. This method is more fundamental than mSSS and, assuming the characteristic impedance and launch admittances can be well controlled, can perform better than mSSS. If the launch admittances are varying (due to switch repeatability, for example), the degradation is more severe if only one line is affected[e.g.,14] and TRL will generally be more affected than mTRL in this case. An example of this launch admittance sensitivity (about 50 fF on one line) is shown in Figure 10 where four lines were used for mTRL. The standards area required for mTRL is about twice that for mSSS for a given bandwidth and sensitivity coverage. The area required may be a limiting factor considering the small volume typically available in the mK zone.

4 Second-tier de-embedding choices

Additional complications come into play when the DUT interface is different from a convenient interface for creating calibration standards (and switching). Examples of the DUT interface may include bonded die, flipchip mounts, spring-loaded contact mounts, etc. If one or two simple standards can be implemented at the DUT interface plane, then a second tier approach may be appropriate to remove the effects of the network between the calibration plane and the DUT plane (see Figure 11).

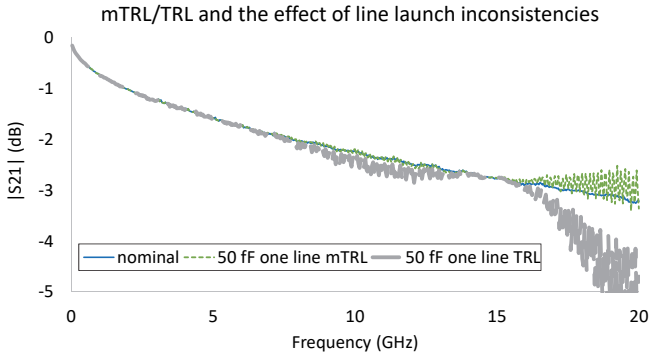

Figure 10 The effect of a changing launch parasitic capacitance on the calibrated insertion loss measurement of a DUT is shown here. When one line is deviant, mTRL can be less sensitive than TRL.

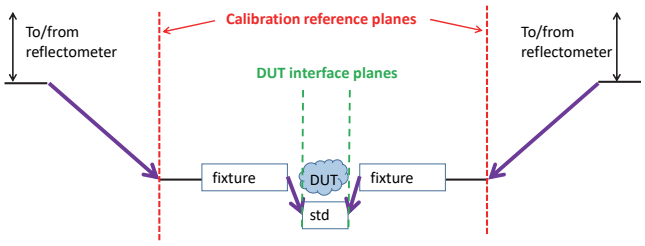

Figure 11 Second tier de-embedding structure where the 'fixture' may include transmission lines, bond wires, and package interfaces.

Generally the standards at the DUT plane are more difficult to implement and only a single short, open or interconnecting line may be possible. Many algorithms exist to handle this class of problem[e.g., 15)-20)] and the choice may be dictated by the length scales involved and the repeatability at the interfaces. Assuming the latter is poor, one class based on using defect localization[e.g., 18),20)] has some advantages in that a single standard can be used and symmetry and geometrical assumptions about the paths are used to help solve for the fixture. Barring such an approach, an alternative may be to fully characterize the interfacial path separately and then reinsert into the mK environment but the repeatability penalties are often large. An example of this tendency, which is dependent of the details of the interfaces, is shown in Figure 12. The most basic approach, ignoring the extra path (fixture) entirely, leads to a maximum error of nearly 2 dB and will often be a last-resort selection. The pre-characterization approach leads to a maximum error of ~0.5 dB while the inline real-time partial information approach had a maximum error of ~0.2 dB.

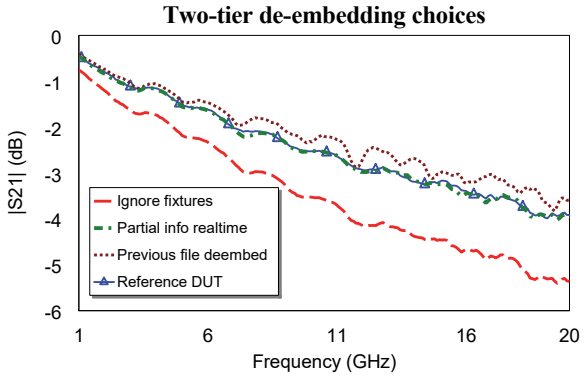

Figure 12 Real-time second-tier de-embedding can sometimes yield better results than multi-step characterizations when the repeatability is not good.

There is a dependence of the two-tier performance on the underlying quality of the primary calibration and this relationship can be complicated. In the next example, the base calibration was distorted in terms of source match and reflection tracking by effectively adding 50 fF launch admittance (as if a spring tip landed differently). In this particular case, both second tier methods of Figure 12 were affected (more than 2x the maximum error) but the frequency dependencies were different because of how the new measurements interacted with the raw DUT data and the 2nd tier measurements.

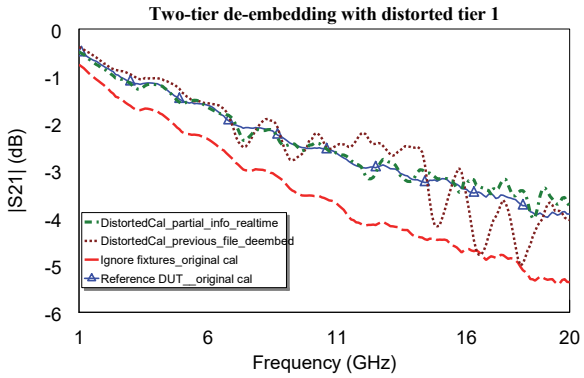

Figure 13 The sensitivity of a second tier de-embed to problems in the underlying calibration can be dependent on the methods employed.

There is still an advantage to the real-time second-tier approach in this second example but understanding the interplay between the de-embedding method chosen, the setup repeatability, and the underlying calibration method is important.

5 Conclusions

In a low-repeatability, high loss environment such as is often encountered in millikelvin network analysis, the signal separation structure often changes and the balance between instrumentation linearity and signal-to-noise ratio may shift. Calibration and de-embedding algorithmic choices may be altered because of standards availability and are also assessed through the lens of a repeatability-challenged environment.

References

1) A. Wallraff, et al, "Strong coupling of a single photon to a superconducting qubit using circuit quantum electrodynamics," *Nature,* vol. 431, pp. 162-167, July 2004.

2) J. C. Bardin, D. J. Slighter, and D. J. Reilly, "Microwaves in quantum computing," *IEEE J. of Micr.,* vol. 1, pp. 403-427, Jan. 2021.

3) D. J. Reilly, "Challenges in scaling-up the control interface of a quantum computer," *2019 IEEE Intl. Elec. Dev. Meeting.*, Oct. 2019, pp. 1-4.

4) A. Akturk, et al, "Compact and distributed modeling of cryogenic bulk MOSFET operation," *IEEE Trans. Elec. Dev.*, col. 57, pp. 1334-1342, June 2010.

5) L. D. Castillo, et al, "Electronic packaging and passive devices for low temperature space applications," *2018 IEEE Aerospace Conf. Proc..*, Sept. 2018, pp. 1-13.

6) .C. R. H. McRae, "Measurement techniques for superconducting microwave resonators towards quantum device applications," *2022 IEEE Int. Micr. Symp. Dig.,* June 2022., pp. 1-3.

7) L. Ranzani, L. Spietz, Z. Popovic, and J. Aumentado, "Two-port microwave calibration at millikelvin temperatures," *Rev, of Sci. Instr.*, vol. 84, pp. 1-9 , Mar. 2013.

8) J. Martens, "De-embedding and calibration in high loss environments," *2022 Eur. Micr. Conf. Wkshp WS07: Microwave design and metrology for quantum computing*, Sept. 2022.

9) M. Stanley, S. E. de Graff, T. Lindstrom, M. J. Salter, J. Skinner, and N. M. Ridler, "Design of microwave calibration standards for characterising S-parameters of quantum integrated circuits at millikelvin temperatures," *2021 EuMW Conf. Dig.*, Apr. 2022, pp. 1-4.

10) Y. Peng, A. Ruffino, and E. Charbon, "A cryogenic broadband sub-1 dB NF CMOS low noise amplifier for quantum applications," *IEEE J. Solid State Cir.*, col. 56, pp. 2040-2053, Jul. 2021.

11) J. Martens, "On quantifying the effects of receiver linearity on VNA calibrations," *70th ARFTG Conf. Dig.*, Dec. 2007, pp. 1-6.

12) A. Lewandowski, W. Wiatr, D. Gu, N. Orloff, and J. Booth, "A multireflect-thru method of vector network analyzer calibration," *IEEE Trans. Micr. Theory Techn.*, vol. 65, pp. 905-915, Mar. 2017.
13) R. B. Marks, "A multiline method of network analyzer calibration," *IEEE Trans. Micr. Theory Techn.*, vol. 39, pp. 1205-1215, July 1991.
14) U. Stumper," Uncertainty of VNA S-parameter measurement due to nonideal TRL calibration items," *IEEE Trans. Instr. And Meas.*, vol. 54, pp. 676-679, Apr. 2005.
15) R. Bauer and P. Penfield, "De-embedding and unterminating," *IEEE Trans. Micr. Theory Techn.*, vol. 22, pp. 282-288, Mar. 1974.
16) J. Wang, R. Groves, B. Jagannathan, and L. Wagner, "Experimental analysis of on-wafer de-embedding techniques for RF modeling of advanced RFCMOS and BiCMOS technologies," *69th ARFTG Conf. Dig.*, June 2007, pp. 1-4.
17) G. F. Engen, "An evaluation of the 'back-to-back' method of measuring adaptor efficiency," *IEEE Trans. Instrum. Meas.*, vol. 19, pp. 18-22, Feb. 1970.
18) H. Barnes, et al, "Performance at the DUT: techniques for evaluating performance of an ATE system at the device under test socket," *DesignCon 2008 Proc.*, Feb. 2008, pp. 1-12.
19) J. Martens, "Common adapter/fixture extraction techniques: sensitivities to calibration anomalies," *74th ARFTG Conf. Dig.*, Dec. 2009, pp. 1-10.
20) J. Martens, "MM-wave partial information de-embedding: errors and sensitivities," *91st ARFTG Conf. Dig.,* June 2018, pp. 1-5.

Author

Jon Martens
Service Infrastructure Solutions
US Division
Test & Measurement Company

Publicly available